ELSEVIER

Polymer 43 (2002) 6985–6992

polymer

www.elsevier.com/locate/polymer

Multicomponent blends based on polyamide 6 and styrenic polymers: morphology and melt rheology

S.H. Jafari[a], P. Pötschke[a,*], M. Stephan[a], H. Warth[b], H. Alberts[b]

[a]*Institute of Polymer Research, Hohe Strasse 6, D-01069 Dresden, Germany*
[b]*Bayer AG, Plastics Business Group, Research and Development Styrenics, D-41538 Dormagen, Germany*

Abstract

The role of each blend component on blend morphology and melt rheological properties was investigated for multicomponent compatibilized blends of polyamide 6 (PA6) and acrylonitrile–butadiene–styrene terpolymer (ABS). Blends with PA6 content of 50 wt% were prepared at similar processing conditions on a ZSK 30 twin screw extruder. PA6/styrene–acrylonitrile co-polymer (SAN) blends showed a dispersed morphology with PA6 as matrix. Addition of reactive compatibilizer, styrene–acrylonitrile–maleic anhydride co-polymer (SANMA), up to 5 wt%, changed the morphology from a dispersed to a co-continuous structure. PA6/ABS, having a part of the SAN substituted by rubber, exhibited a coarse co-continuous structure which could be explained with the yield stress of the ABS. Addition of the compatibilizer to this system refined the co-continuous structure and increased the viscosity as well as the elasticity. © 2002 Elsevier Science Ltd. All rights reserved.

Keywords: Polyamide 6/acrylonitrile–butadiene–styrene terpolymer compatibilized blend; Morphology; Melt rheology

1. Introduction

Multicomponent compatibilized blends of polyamide 6 (PA6) with acrylonitrile–butadiene–styrene terpolymer (ABS) are of high commercial interest as high performance alloys owing to their excellent potential for applications where super tough materials with high thermal stability, good chemical resistance and excellent dimensional stability are required. On the other hand, the ease of processing and stability of the blend over wide processing conditions make this blend suitable for engineering applications [1–4]. Main application areas of the blend are automotive interior components, power tools, garden equipment, sport goods, medical equipment and furniture. PA6 with its highly polar amide groups is not compatible with ABS, therefore, it is necessary to use a functionalized compatibilizer to enhance the interfacial properties between these polymers [5–8]. The reactive groups should easily react with amine end groups to form PA6 grafted co-polymers during the reactive melt blending. On the other hand, physical interactions between the common groups in the ABS and the compatibilizer, result in a very effective compatibilization. In order to find out the effect of each blend component and particularly of the compatibilizer (styrene–acrylonitrile–maleic anhydride co-polymer (SANMA)) on morphological and rheological properties of the blends, four different blends, namely, PA6/styrene–acrylonitrile co-polymer (SAN), PA6/SAN/SANMA, PA6/ABS and PA6/SANMA were extruded under similar processing conditions [5]. These blends are considered as simpler version of the commercially important PA6/ABS/SANMA blend which has several components such as SAN, SAN-*g*-polybutadiene (SAN-*g*-PB) and SANMA co-polymers, themselves consisting of several components.

2. Experimental

All the materials (Polyamide 6 Durethan B29, SAN Lustran M80, ABS Novodur Graft (SAN-*g*-PB) and SANMA) supplied by Bayer AG were in pellet form except for SAN-*g*-PB which was delivered in a powder form. These materials were used for melt blending from air sealed bags without any further treatment.

The blends were prepared on a ZSK 30 twin screw extruder (*L*/*D* ratio of 41) with simultaneous feeding of all blend components at one feeding point (common melting). Prior to melt blending the SAN and SANMA were dry blended and fed through a single feeder. ABS was produced

* Corresponding author. Tel.: +49-351-4658-395; fax: +49-351-4658-565.
E-mail address: poe@ipfdd.de (P. Pötschke).

0032-3861/02/$ - see front matter © 2002 Elsevier Science Ltd. All rights reserved.
PII: S0032-3861(02)00614-6

in situ by simultaneous addition of SAN and the SAN-*g*-PB during the extrusion process. The processing temperature of 260 °C, feeding rate of 10 kg/h, a unique screw and barrel configuration and screw speed of 200 rpm were used for all blends preparation. The melt strands were quenched by passing them through a water bath at room temperature and then chopped to pellets. Two non-reactive uncompatibilized binary blends, namely PA6/SAN, and PA6/ABS, as well as two reactive compatibilized ternary blends, namely PA6/SAN/SANMA, and PA6/ABS/SANMA, were made with an identical blend composition (keeping PA6 content constant at 50 wt%). The compatibilizer level was less than 5 wt% of the total blends. In addition to these series of blends, a binary reactive blend of PA6/SANMA was produced under similar processing conditions in which the blending ratio was kept similar to that of the ternary blends. This blend was used to study the individual effect of SANMA on PA6 properties.

Scanning electron microscopy (SEM) was used to study the morphology of extruded blend strands. The smooth surface obtained by a steel knife on a rotational microtom (Jung RM 2055, Leica) was etched in formic acid for 4 h in order to remove the polyamide phase of the blends or in tetra hydrofuran (THF) for 24 h to etch out the SAN component. The samples were hanged into the solvents within about 2–5 mm. The etched surface after proper drying was gold sputtered and observed under a LEO 435 VP (LEO Elektronenmikroskopie, Germany) SEM. The digitized images were recorded at different magnifications.

Melt rheological investigations were conducted by an ARES Rheometer (Advanced Rheometric Expansion System, Rheometric Inc.) in parallel plates oscillation mode on granulated and properly dried samples. Frequency sweeps of 0.1–100 rad/s were performed at temperature of 260 °C and strain of 5% in N_2 atmosphere.

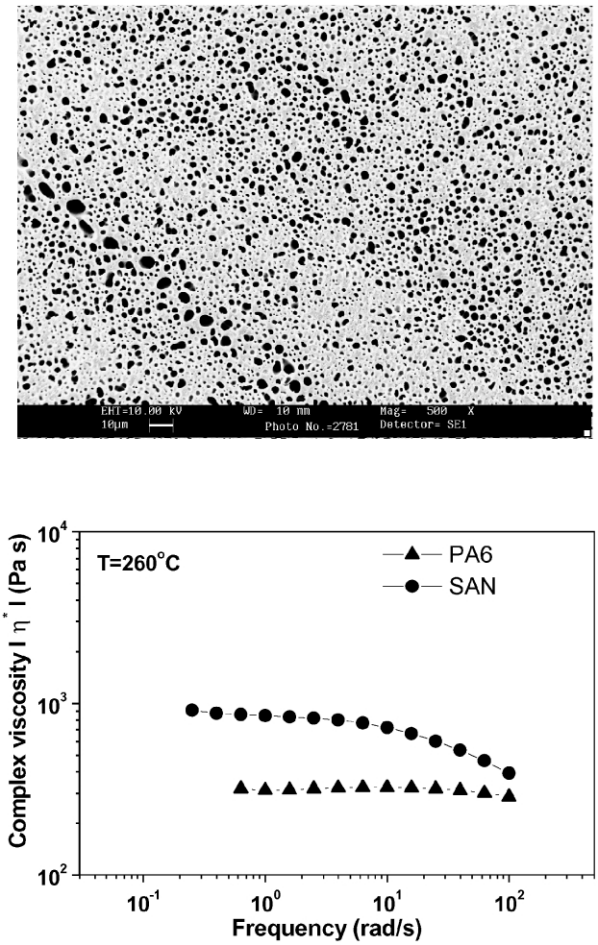

Fig. 1. SEM micrograph of PA6/SAN etched surface in THF illustrating the SAN domains dispersed in the PA6 matrix, along with comparison of the complex viscosities of the blend components (PA6 and SAN).

3. Results and discussion

3.1. Morphology of the blends

3.1.1. PA6/SAN blend

The morphology of the etched cut surface of the PA6/SAN binary blend is shown in Fig. 1. THF was used to dissolve the SAN fraction of the blend revealing the PA6 structure. In this blend SAN forms spherical domains uniformly dispersed in the PA6 matrix. These SAN domains are between 1 and 7 μm in diameter. Although the blend contains SAN as the major volumetric component and PA6 as minor component, the PA6 is the component, which forms the matrix. This is due to lower viscosity of PA6 as compared to the SAN.

There are several models to estimate which phase forms the matrix by predicting the phase inversion composition based on the viscosities (η) of the blend components. According to the empirical relationship for prediction of the phase inversion suggested by Avgeropoulos [9] and generalized by Paul and Barlow [10], the phase inversion occurs when the volume ratio is equal to the viscosity ratio between the blend components. For PA6/SAN blend system the relationship can be expressed as

$$\phi_{SAN} = 1/(1 + \eta_{PA6}/\eta_{SAN}) \quad (1)$$

where η and ϕ denote the viscosity and volume fraction of the blend components, respectively.

Utracki [11,12] proposed a model which included intrinsic viscosity [η]. For the PA6/SAN blend system it leads to an expression

$$\phi_{SAN} = (1 - \log(\eta_{PA6}/\eta_{SAN})/[\eta])/2 \quad (2)$$

where the intrinsic viscosity was assumed to be 1.9 for spherical domains.

Metelkin and Blekht [13] developed another approach based on the theory of Tomotika [14] for the instability of a liquid film or cylinder in another liquid. The expression adopted to the PA6/SAN blend system can be written as

$$\phi_{SAN} = 1/(1 + F(\eta_{PA6}/\eta_{SAN}) \times \eta_{PA6}/\eta_{SAN}) \quad (3)$$

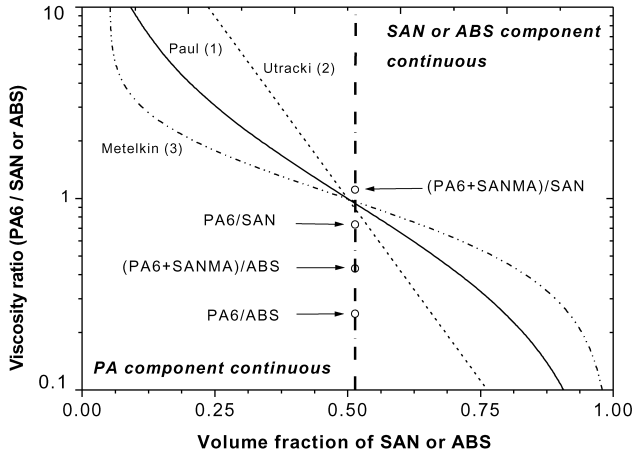

Fig. 2. The predicted phase inversion composition according to the three models.

where F is expressed according to Utracki [12] as:

$$F(\eta_{PA6}/\eta_{SAN}) = 1 + 2.25\log(\eta_{PA6}/\eta_{SAN}) + 1.81[\log(\eta_{PA6}/\eta_{SAN})]^2 \quad (4)$$

The predicted phase inversion composition according to the above three models are shown in Fig. 2. Some other relationships were also proposed by Ho [15], Kitayama [16] and Everaert [17] by modifying Eq. (1) with introduction of some pre-factor or exponents to achieve better fits for their experimental results.

The rheological investigations made by an oscillation rheometer at 260 °C shown in Fig. 1 indicate that the viscosity of PA6 is lower than that of the SAN. The extrapolated zero shear rate viscosity is about 1000 Pa s for SAN and about 300 Pa s for PA6. Assuming the validity of Cox–Merz rule relating steady shear viscosity with the absolute value of complex viscosity [18], the viscosity ratio (η_{PA6}/η_{SAN}) of 0.73 can be estimated at a mean shear rate of 100 s^{-1}. The maximum oscillation frequency of 100 rad/s achievable in the oscillation rheometer can be assumed with a good approximation to be equal to the average shear rates in the ZSK 30 twin screw extruder, although the shear rates can be expected to be 5–5000 s^{-1} during the extrusion process.

Taking into account the viscosity ratio of 0.73 and using Eqs. (1)–(3), the phase inversion point at which the SAN forms the continuous phase or the matrix, is found to be at higher concentration than the actual SAN content of the blend. Therefore, SAN should form the dispersed phase. Thus, according to all the three models, the morphology obtained is in accordance with the expectation based on the viscosity ratio for binary blend of PA6/SAN.

3.1.2. PA6/ABS blend

Fig. 3 shows the morphology of etched cut surface of PA6/ABS blend. As compared to the PA6/SAN blend, here a part of SAN is replaced by the SAN-*g*-PB. For this blend

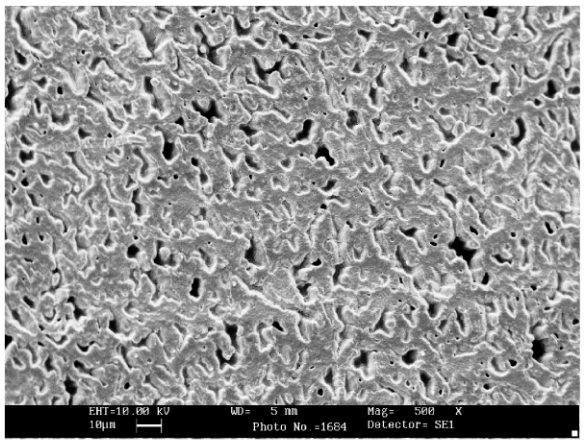

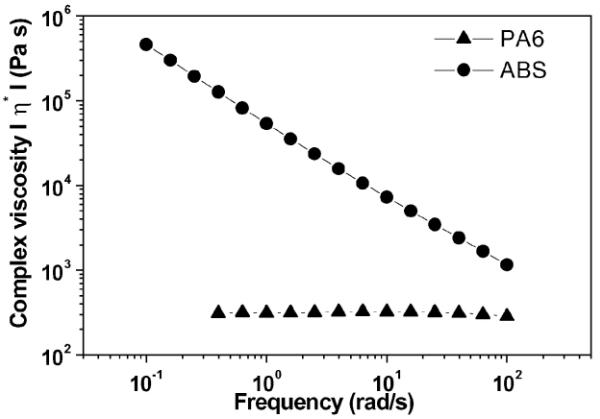

Fig. 3. SEM micrograph of PA6/ABS etched surface in formic acid illustrating a coarse co-continuous structure, along with comparison of the complex viscosities of the blend components (PA6 and ABS).

formic acid was used to etch out the polyamide component hence revealing the remaining ABS structure. The morphology appears coarse co-continuous. To check the co-continuity in addition etching was performed with THF to etch out the SAN fraction. By this procedure it is assumed that the embedded SAN-*g*-PB particles are also removed from the sample surface. An example showing the comparison of surfaces etched in THF and formic acid for a PA6/ABS blend having a slightly different composition is shown in Fig. 4. These morphological investigations indicate that the addition of the rubber to SAN induces a change in the morphology type from a dispersed type to a coarse co-continuous morphology. Looking at the rheology of the blend components one can notice that ABS has much higher viscosity than the SAN. This increase of viscosity is caused by the addition of the rubber particles. Moreover, ABS does not show a Newtonian plateau at low frequencies but a linear increase in viscosity with decreasing the shear rate. It also exhibits a very high elasticity (see G' in Fig. 10b), which determines mainly the complex viscosity.

Using the same procedure to calculate the phase inversion composition by applying Eqs. (1)–(3) for the viscosity ratio (η_{PA6}/η_{ABS}) of 0.25, the ABS phase should

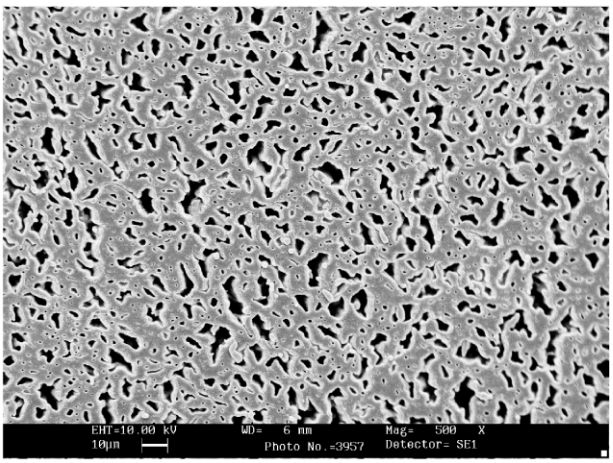

(a)

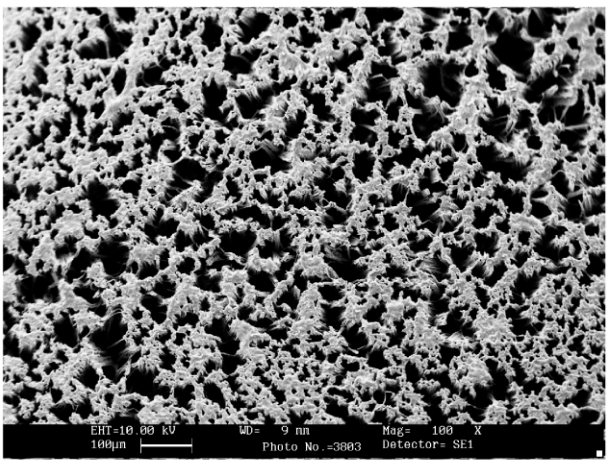

(b)

Fig. 4. SEM micrographs of PA6/ABS blend cut surfaces etched in (a) formic acid; (b) THF, revealing a co-continuous structure.

form the dispersed phase according to all the three models (Fig. 2). Although the actual ABS content is far away from the phase inversion composition ABS exists as a continuous phase. It is well known that there can be a co-continuous region around the phase inversion composition whose composition range depends mainly on the interfacial tension [19]. Low interfacial tension leads to broader co-continuous ranges. By adding rubber particles to SAN the interfacial tension, which is reported by Son [20] for PA6/SAN to be in the range 4.5 mN/m, should not be changed significantly. This indicates that for the PA6/ABS blend such type of morphological prediction by use of the viscosity ratio is not suitable to explain the type of morphology. This could be due to the high elasticity (see G' in Fig. 10b) and the existence of a yield stress of the ABS as evident from the sharp increase of melt viscosity at low frequencies. This rheological behavior is typical for thermoplastic elastomers and filled systems [21]. In some aspects the ABS can be regarded as a rubber filled SAN system. Blends containing such materials which show yield stress are known to form very stable co-continuous structures over a broad composition range [22–26]. In such blends, the thermoplastic elastomer exhibiting the higher viscosity—in our case ABS—and in some cases also a higher surface tension, forms a skeletal structure with convex surfaces. The other components—in this case being PA6—takes up the antitropic co-continuous structure filling the spaces between the skeletal structure [22]. The yield stress prevents the break-up and retraction of this skeletal structure [27] and it is responsible for the special behavior of such type of blends with co-continuous structure [25,26].

3.1.3. PA6/SANMA—role of SANMA

The SANMA, a terpolymer of styrene, acrylonitrile, and maleic anhydride, is miscible with the SAN or the SAN part of ABS. On the other hand, the maleic anhydride segments of this terpolymer which are located at the interface, are capable of reacting with the amine end groups of PA6 known as imidization reaction, forming co-polymers at the interface (Fig. 5).

These interactions result in the stabilization of the interface by reducing the coalescence, reduction of interfacial tension, and enhancing the interfacial viscosity and adhesion. Thus, SANMA can act as an excellent reactive compatibilizer for PA6/ABS blends. In order to estimate the effect of the reaction and the consequent interfacial interactions on the rheological behavior and resulting morphology, a binary reactive blend of PA6/SANMA was made keeping the blending ratio similar to that of the ternary compatibilized blends. Fig. 6 shows a comparison between the melt viscosity of the PA6 with that of binary reactive blend of PA6 with SANMA. The melt viscosity (Fig. 6) and elasticity (see G' in Fig. 9b) increase significantly as a result of the reactive blending. At a shear rate of 100 s^{-1} the viscosity of the PA6/SANMA blend is almost double of the neat PA6.

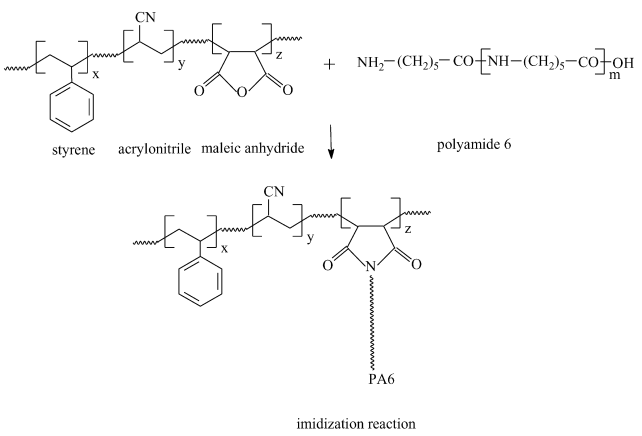

Fig. 5. Interfacial reaction between polyamide 6 and the compatibilizer.

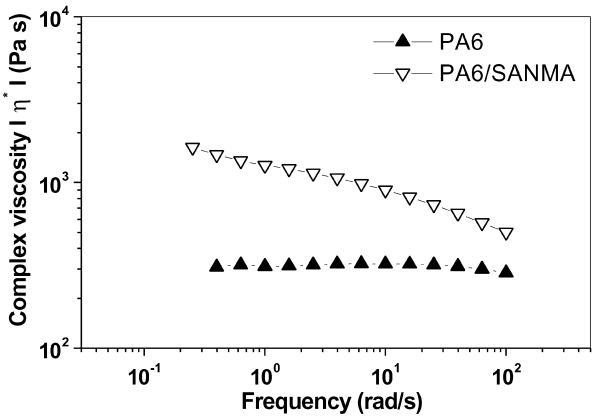

Fig. 6. Comparison of the complex viscosities of PA6 and PA6/SANMA reactive blend.

3.1.4. PA6/SAN + SANMA

This is a reactive compatibilized ternary blend obtained by addition of the SANMA terpolymer to PA6/SAN. Morphology of the cut surface etched by formic acid, hence exposing the SAN structure, is shown in Fig. 7. As compared to the binary non-reactive blend (PA6/SAN) this blend shows a co-continuous structure. The addition of the compatibilizer leads to a change in morphology that is a transition from a dispersed structure to a co-continuous structure occurs.

3.1.5. PA6/ABS + SANMA

Now let us examine the effect of further addition of the rubber component into the reactive PA6/SAN/SANMA system. As discussed earlier by replacing a part of SAN with rubber grafted component (SAN-*g*-PB) in the non-reactive system, a significant increase in melt viscosity and a yield stress were observed which resulted in change of morphology type from a dispersed to a coarse co-continuous structure. For the reactive system containing rubber, addition of the SANMA causes significant refinement of the co-continuous structure as evident from the SEM

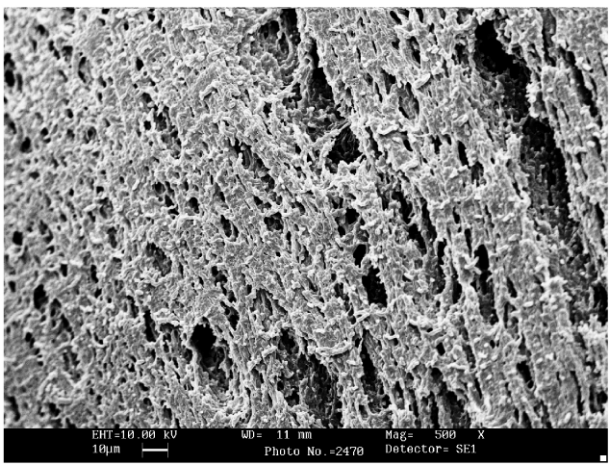

Fig. 7. SEM micrograph of PA6/SAN + SANMA etched surface in formic acid illustrating a co-continuous morphology.

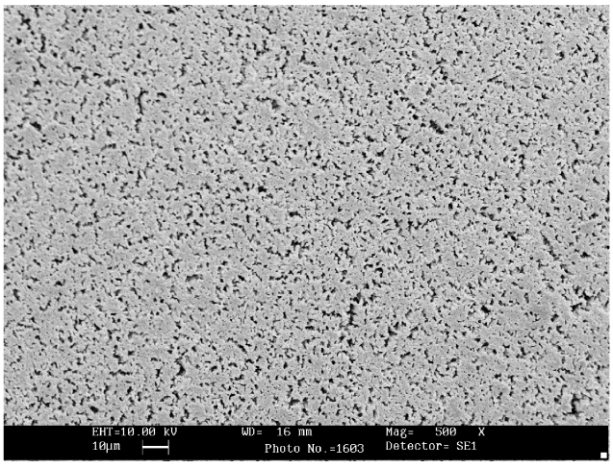

(a)

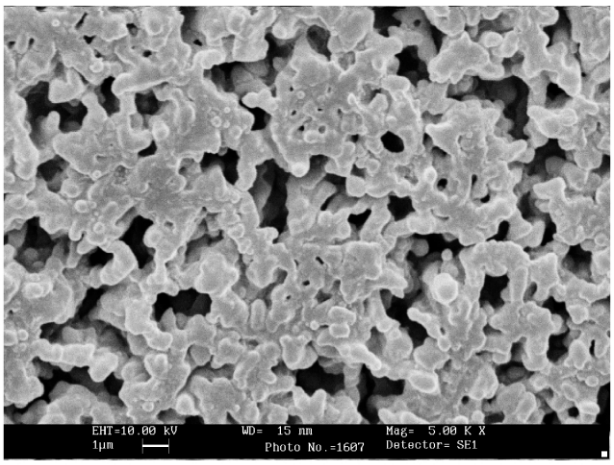

(b)

Fig. 8. SEM micrographs of etched surface in formic acid of PA6/ABS + SANMA (a) at low magnification × 500; and (b) at high magnification × 5000, illustrating the refinement of the co-continuous structure by addition of the reactive compatibilizer to PA6/ABS.

micrographs shown in Fig. 8. This can be explained by the reduced interfacial tension, which stabilizes the interface and the hindered coalescence. In addition, the viscosity ratio between PA6 reacted with SANMA and ABS becomes smaller but still far away from the calculated phase inversion composition (Fig. 2). The skeletal structure is clearly visible in the magnified micrograph.

3.2. Rheological behavior of the blends

3.2.1. PA6/SAN based blends

In this section we investigate how these morphological differences influence the rheological behavior of the blends. Fig. 9a–d presents the melt rheological behavior of the blends containing SAN (both non-reactive and reactive blends) in combination with the pure components. From Fig. 9a one can notice that the melt viscosity of the PA6/SAN blend follows almost a linear mixing rule. This means the viscosity of this blend is in between the viscosities of

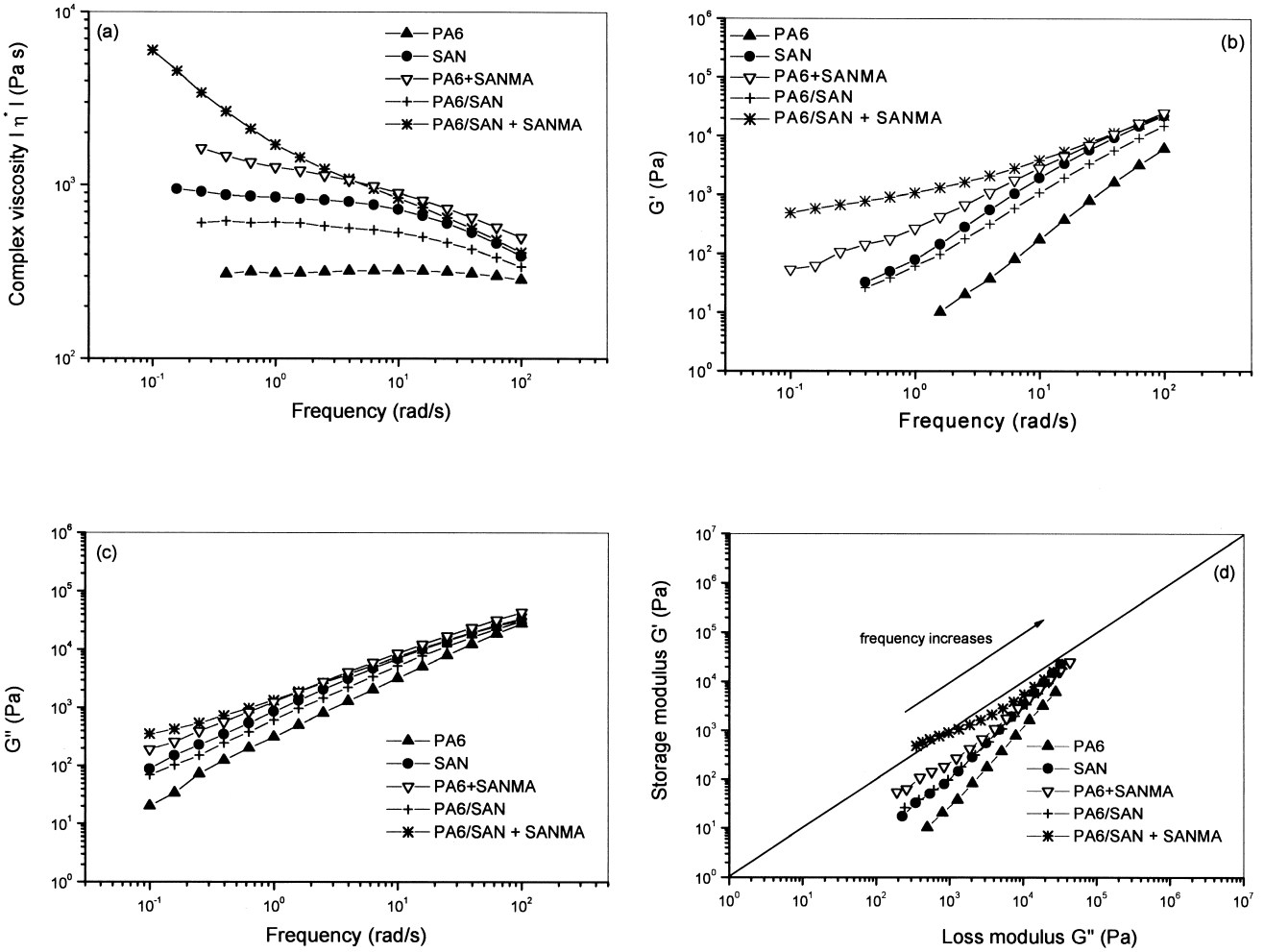

Fig. 9. Rheological behavior of PA6/SAN and PA6/SAN + SANMA along with the blend components (a) complex viscosity; (b) storage modulus (G'); (c) loss modulus (G'') and (d) G' versus G''.

PA6 and SAN neat components. The compatibilized blend (PA6/SAN/SANMA) can be regarded as a blend of PA6 modified with SANMA (PA6/SANMA) and SAN. Its behavior is quite different as compared to the components. At low frequencies this blend shows a significant increase in viscosity. This change in behavior is related to the existence of the co-continuous structure, which can be explained by extra stresses connected with the shape relaxation. This kind of behavior is also reported by some other authors [11,28].

The same relationship exist for both storage modulus G' and the loss modulus G'' as it can be seen in Fig. 9b and c, respectively. The non-reactive blend shows modulus between the constituent components whereas, the reactive compatibilized blend show higher G' and G'' values than those of the constituents components. This effect is more pronounced concerning the elastic properties clearly visible in the storage modulus values. Fig. 9d shows the relationship between the storage modulus and the loss modulus with the frequency as a parameter for the SAN based blends. This kind of plot was introduced by Han [29] in 1983 and later on the plot G'' versus G' was named as modified Cole–Cole plot by Harrel and Nakayama [30,31]. It is seen that at a given G'', the compatibilized blend exhibits the highest values for G' and thus, elasticity, due to its co-continuous structure.

3.2.2. PA6/ABS based blends

The rheological behavior for the PA6/ABS and PA6/ABS + SANMA blends is shown in Fig. 10a–d. One has to consider that these ABS based blends have much higher viscosities than the SAN based blends. As it is seen from Fig. 10a, both the reactive and non-reactive ABS blends show viscosities between the constituents components. The reactive compatibilized blend can be considered as a combination between PA6 modified with SANMA and the ABS. Viscosities of the both ABS blends, reactive and non-reactive ones, are higher than the values expected by application of a linear mixing rule. The blends show a linear increase in viscosity with decreasing frequency, indicating the existence of a yield stress not only in the ABS but also in the blends based on ABS. Similar to the previous system, here also these changes are

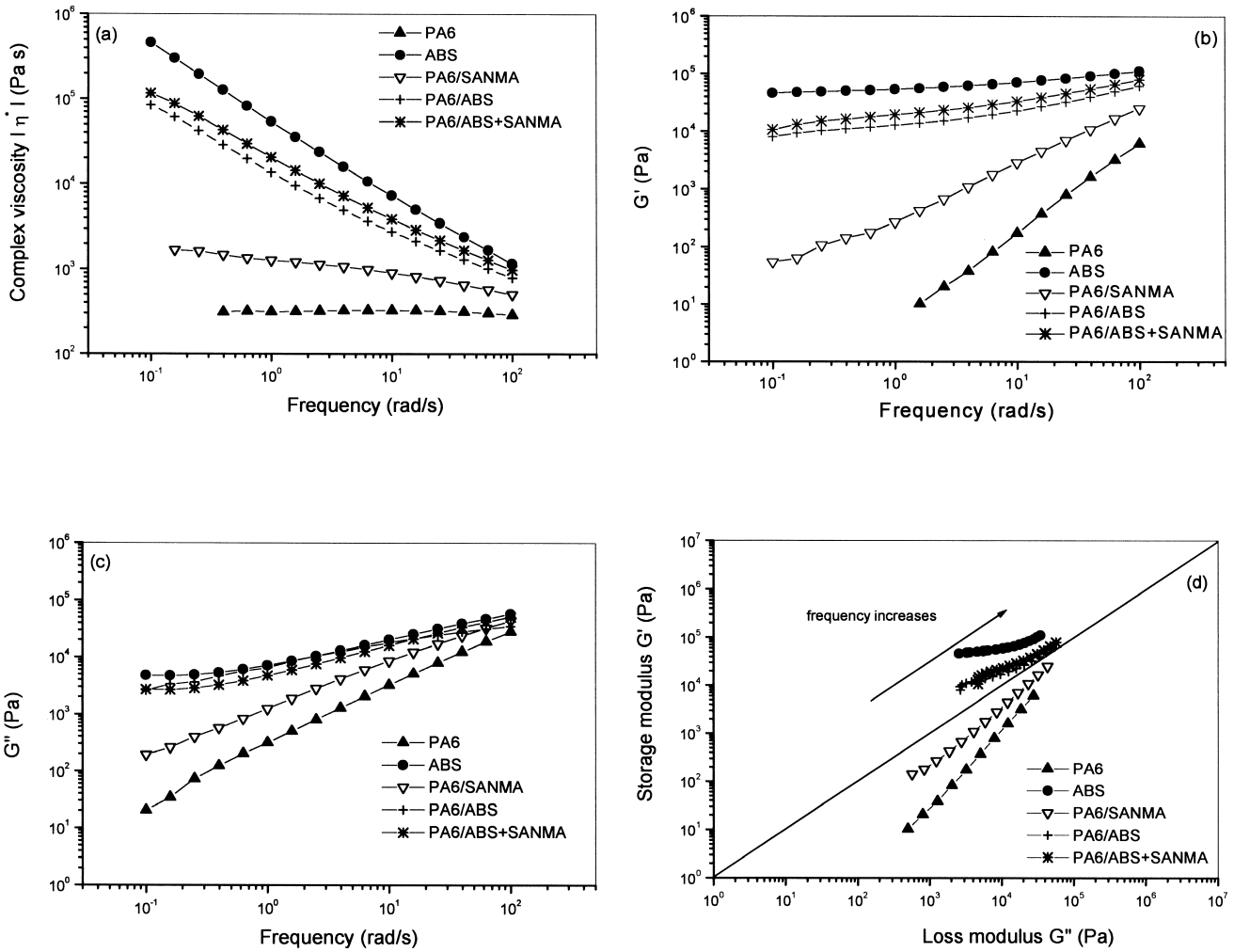

Fig. 10. Rheological behavior of PA6/ABS and PA6/ABS + SANMA along with the blend components (a) complex viscosity; (b) storage modulus (G'); (c) loss modulus (G'') and (d) G' versus G''.

more pronounced in G' as compared to the G'' values (Fig. 10b and c). The plot of G' versus G'' (Fig. 10d) indicates that both the compatibilized and uncompatibilized ABS blends have the same qualitative microstructure (co-continuous), as the curves are nearly the same for both the blends.

4. Conclusions

This systematic study was carried out to understand the complex nature of the commercially important compatibilized PA6/ABS multicomponent blend. For this purpose, blends of PA6 with SAN and ABS, with and without compatibilizer, having PA6 content of 50 wt%, were investigated. The approach was to start with a binary blend of PA6/SAN and to add additional components one by one to reach to the final blend formulation. The effect of addition of SAN, the grafted rubber component (SAN-*g*-PB), the compatibilizer and the overall combined effects on the blend morphology and the melt rheology were studied. PA6/SAN blend showed a dispersed morphology with PA6 as matrix. Addition of the reactive compatibilizer led to a significant change in morphology to a co-continuous structure. The resulting changes in the melt rheological properties were also dramatic. The increase in viscosity at low frequencies indicated the existence of the co-continuous structure. PA6/ABS exhibited a coarse co-continuous structure. The formation of the co-continuous structure could not be explained based on the viscosity ratios of the components but seemed to be connected with the yield stress of the ABS due to its rubber component. Addition of the reactive compatibilizer to this system refined the co-continuous structure and increased the viscosity as well as the elasticity.

References

[1] de Clercq Zubli M, Verhooren P. Kunstst Plast Eur 1997;87(12): 19–20.
[2] Dunning L. Kunststoffe 1996;86(1):98–100.
[3] Henton DE, Mang MN. US Patent 5,089,557; February 18, 1992.

[4] Triax® blends of ABS and polyamide. Bayer engineering thermoplastic: products and applications. Edition 1/98. p. 47–51.
[5] Jafari SH, Pötschke P, Stephan M, Pompe G, Warth H, Alberts H. J Appl Polym Sci 2002;84(14):2753–9.
[6] Kudva RA, Keskkula H, Paul DR. Polymer 2000;41:239–58.
[7] Kudva RA, Keskkula H, Paul DR. Polymer 1998;39(12):2447–60.
[8] Lacasse C, Favis BD. Adv Polym Technol 1999;18:255–67.
[9] Avgeropoulos GN, Weissert FC, Biddison PH, Böhm GGA. Rubber Chem Technol 1976;49:94.
[10] Paul DR, Barlow JW. J Macromol Sci, Rev Macromol Chem 1980; C18(1):109–68.
[11] Utracki LA. J Rheol 1991;35:1615–37.
[12] Utracki LA. Polym Mater Sci Engng 1991;65:50–1.
[13] Metelkin VI, Blekht VP. Colloid J USSR 1984;46:425–9.
[14] Tomotika S. Proc R Soc Lond, Ser A 1935;150:322.
[15] Ho RM, Wu CH, Su AC. Polym Engng Sci 1990;30:511–8.
[16] Kitayama N, Keskkula H, Paul DR. Polymer 2000;41:8041–52.
[17] Everaert V, Aerts L, Groeninckx G. Polymer 1999;40:6627–44.
[18] Cox WP, Merz EH. J Polym Sci 1958;28:619–21.
[19] Willemse RC, Posthuma de Boer A, van Dam J, Gotsis AD. Polymer 1999;40:827–34.
[20] Son Y. Polymer 2000;42:1287–91.
[21] Shenoy AV, Rheology of filled polymer systems. Dordrecht, The Netherlands: Kluwer; 1999.
[22] Gergen WP. Kautsch Gummi Kunstst 1984;37:284–90.
[23] Veenstra H, van Dam J, Posthuma de Boer A. Polymer 2000;41: 3037–45.
[24] Veenstra H, van Lent B, van Dam J, Posthuma de Boer A. Polymer 1999;40:6661–72.
[25] Veenstra H, van Dam J, Posthuma de Boer A. Polymer 1999;40: 1119–30.
[26] Gergen WP, Lutz RG, Davison S. Hydrogenated block copolymers in thermoplastic elastomer interpenetrating polymer networks. In: Holden G, Legge NR, Quirk R, Schroeder HE, editors. Thermoplastic elastomers, 2nd ed. Munich: Hanser; 1996.
[27] Elmendorp JJ. Polym Engng Sci 1986;26(6):418–26.
[28] Steinmann S, Gronski W, Friedrich C. Rheol Acta 2002;41:77–86.
[29] Han CD, Lem KW. Polym Engng Rev 1983;2:135–65.
[30] Harrell ER, Nakayama N. J Appl Polym Sci 1984;29:995–1010.
[31] Nakayama N, Harrell ER. Modified Cole–Cole plot as a tool for rheological analysis of polymers. In: Ottenbrite RM, Utracki LA, Inoue S, editors. Current topics in polymer science. Rheology and polymer processing/multiphase systems, vol. II. Munich: Hanser; 1987. p. 149–65.